HEMI-CYLINDER UNWRAPPING ALGORITHM OF FISH-EYE IMAGE BASED ON EQUIDISTANT PROJECTION MODEL

Jingtao Lou, Yongle Li, Yu Liu, Wei Xu, Maojun Zhang

College of Information System and Management, National University of Defense Technology, Changsha 410073, China
loujt_1984@126.com

ABSTRACT

This paper presents a novel fish-eye image unwrapping algorithm based on equidistant projection mode. We discuss a framework to estimate the image distortion center using vanishing points extraction. Then we propose a fish-eye image unwrapping algorithm using hemi-cylinder projection in 3D space. Experimental results show that our algorithm is efficient and effective. In particular, the hemi-cylinder unwrapping results do not reduce the horizontal field of view which is very useful for panoramic surveillance with applications in important sites safety compared with other fish-eye image correction methods.

Index Terms—Equidistant projection, vanishing points, center estimation, hemi-cylinder unwrapping

1. INTRODUCTION

The wide angle cameras containing fish-eye lens are widely used in many applications, including robot navigation, 3D reconstruction, image-based rendering, and single view metrology, because they can provide a large field of view (FOV) with more visual information from a single image. Therefore, fish-eye distortion correction is a foundational key work along with the uses of fish-eye lens, such as video surveillance, etc. Some generic calibration models are published in [1, 2, 3]. Wonpil Yu [4] proposed a distortion correction method using second-order radial distortion model for mobile computing applications. Seok-Han Lee et al. [5] discussed a framework to determine distortion vectors and distortion function directly using a planar checkerboard. There are some other state-of-the-art techniques of camera distortion calibration and correction, such as, Moumen T. El-Melegy et al. [6] presented an automatic approach based on the robust least-median-of-squares (LMS) estimator. Devernay et al. [7] assumed the presence of straight lines in the scene. Distortion parameters are sought which lead to lines being imaged as straight in the undistorted image. In applying camera perspective principles to camera calibration, both Cipolla et al. [8] and Daniilidis and Ernst [9] describe methods using rectilinear pin-hole perspective to extract the principal point, and other camera calibration parameters for rectilinear cameras.

Nevertheless, most of the calibration methods aimed to correct fish-eye image to accord with pin-hole perspective projection principles as close as possible. Moreover, there is always much severe distortion in the margin of undistorted image which may lost some important information in the original image. Our proposed hemi-cylinder unwrapping algorithm has solved this problem properly. And the unwrapping results of fish-eye images are comfortable for human visual observation which also holds the original information as full as possible.

The remainder of this paper is structured as follows: In Sec. 2, we describe the vanishing points extraction of distorted image and estimate the distortion center. Next in Sec. 3, a novel hemi-cylinder unwrapping algorithm of fish-eye image based on equidistant projection model is presented in detail. The experimental results are given in Sec. 4. Finally, Sec. 5 concludes this article.

2. RELATED WORK

In this section, an image calibration technique employed for the estimation of distortion center making use of vanishing points extraction method is described. Firstly, equidistant projection model and analysis of vanishing points extraction are proposed in theory. Then, we give the result of distortion center estimation using circle fitting.

2.1. Equidistant projection

Equidistant projection model [10] is used very commonly in the analysis of fish-eye lens distortion. It has a nonlinear and radial distortion which is described in Fig. 1.

This research was partially supported by National Natural Science Foundation (NSFC) of China under project No.61175006, No.61175015, No.61271438, and No.61275016; iCORE (Alberta Innovates) Alberta, and NSERC Canada.

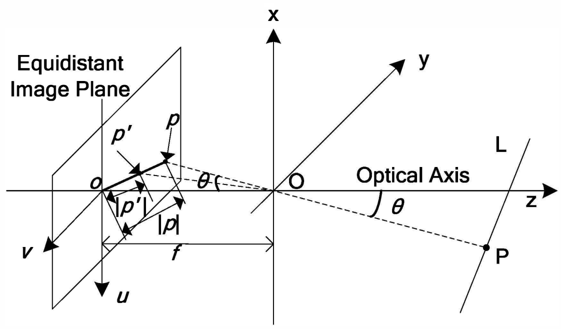

Fig. 1. Sketch map of equidistant projection model

Where, $|p'|$ is the radial distance from point p' to the distortion center, given by

$$|p'| = f \bullet \theta \tag{1}$$

Generally, a line in 3D space can be described as

$$P(t) = Et + R \tag{2}$$

Where, $E = [E_x, E_y, E_z]^T$ is the unit direction vector of the line L, $R = [R_x, R_y, R_z]^T$ is a point through which the line passes and t is the distance parameter that describes any given point on the line. The conversion between the undistorted image radial distance and distorted image radial distance described is obtained by solving in terms of θ and has

$$|p| = f \bullet \tan\frac{|p'|}{f},\ p = \frac{|p|}{|p'|}p' \tag{3}$$

And it also has

$$|p'| = f \bullet \arctan\frac{|p|}{f},\ p' = \frac{|p'|}{|p|}p \tag{4}$$

This describes the conversion from a point on the undistorted rectilinear image plane to the distorted equidistant image plane. Thus, if we take (2) as the projection of a straight line on to the rectilinear image plane, and apply distortion using (1), we get the following equations (5) and (6) to describe the projection of a 3D straight line on to the distorted image plane

$$p'(t) = [E_x t + R_x, E_y t + R_y]^T \frac{|p'(t)|}{|p(t)|} \tag{5}$$

$$\frac{|p'(t)|}{|p(t)|} = \frac{f \arctan\left(\frac{\sqrt{(E_x t + R_x)^2 + (E_y t + R_y)^2}}{E_z t + R_z}\right)}{\sqrt{(E_x t + R_x)^2 + (E_y t + R_y)^2}} \tag{6}$$

To find the vanishing point $v' = [v'_u, v'_v]^T$ of the projection of 3D parallel lines to the distorted image plane which shows in Fig. 2, the limit of $p'(t)$ as $|t| \to \infty$ is found. And the vanishing points are

$$v' = \lim_{|t|\to\infty} p'(t) = [E_x, E_y]^T \lim_{t\to\pm\infty} \frac{|p'(t)|}{|p(t)|} \tag{7}$$

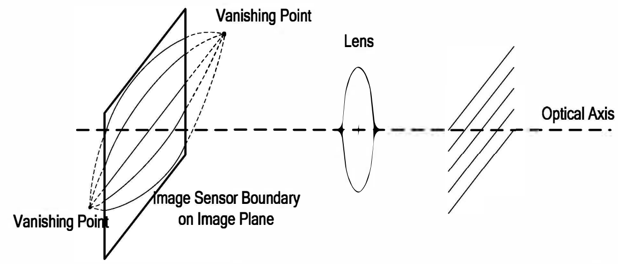

Fig. 2. Sketch map of vanishing points of a projected set of parallel lines in equidistant projection

Describing the equidistant projection of straight lines is more complex, and attempting to fit image data to these equations could prove both costly and complex. It would be far more desirable if projected lines could be fit to some simpler geometric shape. C. B. Burchardt and K. Voss [11], etc. suggest that the projection of straight lines in cameras exhibiting radial distortion results in circles on the image plane.

2.2. Vanishing points extraction

In the previous section, we have shown how the equidistant projection of 3D straight lines can be approximated as arcs of circles, and that a set of projected parallel 3D lines converge at two vanishing points on the image plane. The method we use to extract vanishing points relies on the use of a planar checkerboard pattern, which is often used for the conventional camera calibration technique.

If circles can be used to estimate the projection of a straight line on to the equidistant image plane, the method of fitting a function to the data is simpler. In this case, the model consists of two vanishing points [12]. For each pair of lines, circles are fit to the projected lines, and their intersection points are determined (their putative vanishing points). The support of each edge in the image for the putative vanishing points is found by the LMS fitting of circles through the edge points, and forcing the fitted circle through the vanishing point pair, by minimizing the error function

$$error = \sum_{i=1}^{N}((u_i - u_0)^2 + (v_i - v_0)^2 - R^2)^2 \tag{8}$$

Where, $[u_0, v_0]^T$ is the center and R is the radius of the fitted circle. Clearly, the lower the returned error, the more support a given edge has for the putative vanishing point pair.

2.3. Distortion center estimation

Up until now, we have assumed that the origin of the image plane is at the distortion center. Of course, that is not practical, as the distortion center may not be known and therefore cannot be used as the origin of the image coordinate system. The estimation of the vanishing points in the previous section via minimization of the error of circle fits to the data are applied to calibration images from which a line can be created as the line that joins the two vanishing points. As was demonstrated in Section 2.2, these lines both intersect the distortion center. Therefore, the distortion center can be estimated as the point at which the two lines cross.

3. HEMI-CYLINDER UNWRAPPING ALGORITHM

In this work, we present a novel fish-eye image hemi-cylinder unwrapping algorithm. The unwrapping results are more comfortable for human visual observation compared with other correction methods. And experimental results will be showed in next section.

A. Projection mapping relationship between $p(x_p, y_p, z_p)$ in hemi-cylinder plane and $p'(x_f, y_f)$ in image plane (according to Fig. 3).

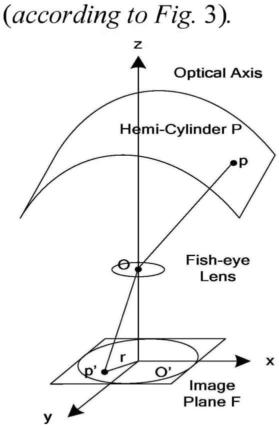

Fig. 3. Equidistant projection sketch map of p in hemi-cylinder plane P the p' in image plane F in 3D space

$p'(x_f, y_f)$ in the image plane F is the equidistant model projection of $p(x_p, y_p, z_p)$ which is in the plane of hemi-cylinder *P* in 3D space as shown in Fig. 3.

As known in the 3D space and the equidistant projection model, the point-to-point relationship in both planes is calculated. In fish-eye image plane F, It can be described as

$$\begin{cases} x_f = r\cos\varphi_p = f\theta\cos\varphi_p \\ y_f = r\sin\varphi_p = f\theta\sin\varphi_p \end{cases} \tag{9}$$

The angle between line op and z-axis

$$\theta = \arctan\left(\frac{\sqrt{x_p^2 + y_p^2}}{z_p}\right) \tag{10}$$

The angle between line op and x-axis:

$$\varphi_p = \arccos\left(\frac{\sqrt{x_p^2 + y_p^2}}{x_p}\right) \tag{11}$$

So, from equations (9), (10) and (11), the coordinates of point $p'(x_f, y_f)$ in the fish-eye image plane are

$$\begin{cases} x_f = f\left(\arctan\left(\frac{\sqrt{x_p^2 + y_p^2}}{z_p}\right)\right)\cos\left(\arccos\left(\frac{\sqrt{x_p^2 + y_p^2}}{x_p}\right)\right) \\ y_f = f\left(\arctan\left(\frac{\sqrt{x_p^2 + y_p^2}}{z_p}\right)\right)\sin\left(\arccos\left(\frac{\sqrt{x_p^2 + y_p^2}}{x_p}\right)\right) \end{cases} \tag{12}$$

B. Projection mapping relationship between $p(x_p, y_p, z_p)$ in hemi-cylinder plane and $t(x_t, y_t)$ in unwrapping plane (according to Fig. 4).

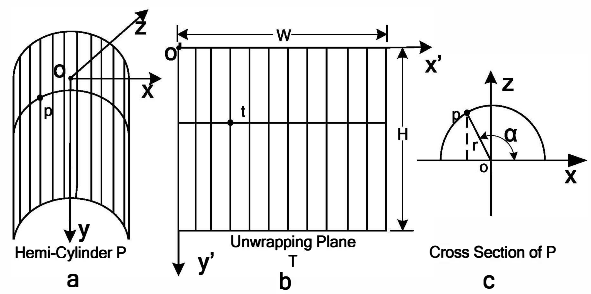

Fig. 4. Corresponding projection relationship of the points between unwrapping plane T and hemi-cylinder plane P

As shown in Fig. 4, W is the width of the unwrapped image which is defined as a constant, and H is the height of the unwrapped image which is the same as the height of fish-eye image. According to the corresponding relationship between the point *p* in the hemi-cylinder P and the point $t(x_t, y_t)$ in the unwrapping plane T, we can obtain the correction result of distorted fish-eye image.

Apparently

$$y_p = y_t \tag{13}$$

and

$$x_p = r\cos(\alpha), \quad z_p = r\sin(\alpha) \tag{14}$$

where

$$\alpha = \frac{(W - x_t)}{W}\pi, \quad r = \frac{W}{\pi} \tag{15}$$

Lastly, we calculate the mapping relationship between the fish-eye image F and the hemi-cylinder unwrapping plane T to create a lookup table.

4. EXPERIMENTAL RESULTS

4.1. Hardware platform

With the application in video surveillance, the TMS320DM368 processor of TI (Texas Instruments) is applied in our experimental system. The image sensor is Aptina Micron MT9P031 and the lens is DW1634D of DAIWON Optical Co. Ltd.. The hemi-cylinder unwrapping algorithm is embedded into the IP camera which we design by the hardware above. In order to save the hardware resources, only one quarter size of the lookup table is required. We take the full advantage of symmetry in hemi-cylinder unwrapping algorithm.

4.2. Image unwrapping results

A. Hemi-cylinder unwrapping results

Fig. 5 shows the experimental results of the proposed hemi-cylinder unwrapping method for two images taken by our hardware platform in different scenes which are outdoor and indoor respectively. Fig. 5-(a) and (c) are the original fish-eye images. Fig. 5-(b) and (d) are the results after the proposed method has been applied.

Outdoor

(a) (b)

Indoor

(c) (d)

Original fish-eye image   Hemi-cylinder unwrapping output

Fig. 5. Hemi-cylinder unwrapping results.

B. Comparative experimental results

For the comparison with the previous approach, some comparative results are illustrated in Fig.6. In particular, we compared experiment results based on our algorithm to the method described in Seok-Han Lee [5]. The experimental results verify that the proposed method is effective to handle with the lens distortion problem, and does not reduce the horizontal FOV which is very useful for panoramic surveillance with applications in important sites safety.


(a) Original fish-eye image


(b) Hemi-cylinder method   (c) Lee's method

Fig. 6. Comparative experimental results.

5. CONCLUSION AND FUTURE WORK

We discuss a new hemi-cylinder unwrapping algorithm to correct fish-eye image distortion. Firstly, we describe the equidistant fish-eye perspective in terms of the projection of sets of parallel lines to the equidistant fish-eye plane and a set of 3D parallel lines converge at two vanishing points on the equidistant image plane. Then we estimate the image distortion center using vanishing points extraction. Experimental results show that our algorithm is efficient and effective. We believe that the proposed scheme can be employed as a useful tool in the camera-lens related works.

REFERENCES

[1] J. Kannala, S. S. Brandt, "A generic camera model and calibration method for conventional, wide-angle, and fish-eye lenses," IEEE Transactions on Pattern Analysis and Machine Intelligence, vol. 28, no. 8, pp.1335-1340, 2006.

[2] Y. Li, M. Zhang, Y. Liu and Z. Xiong, "Fish-eye distortion correction based on midpoint circle algorithm," IEEE International Conference on Systems, Man, and Cybernetics, pp. 2224-2228, 2012.

[3] J. Wei, C. F. Li, S. M. Hu, R. R. Martin and C. L Tai, "Fisheye video correction," IEEE Transactions on Visualization and Computer Graphics, vol. 18, no. 10, pp. 1771-1783, 2012.

[4] W. Yu, "An Embedded Camera lens distortion correction method for mobile computing applications," IEEE Transactions on Consumer Electronics, vol. 49, no. 4, pp.894-901, 2003.

[5] S. H. Lee, S. K. Lee, "Correction of radial distortion using a planar checkerboard pattern and its image," IEEE Transactions on Consumer Electronics, vol. 55, no. 1, pp.27-33, 2009.

[6] M. T. El-Melegy, A. A. Farag, "Nonmetric lens distortion calibration: closed-form solutions, robust estimation and model selection," Proceedings of IEEE International Conference on Computer Vision, 2003.

[7] F. Devernay, O. Faugeras, "Straight lines have to be straight," Machine Vision and Applications, vol. 13, no. 1, pp.14-24, 2001.

[8] R. Cipolla, T. Drummond, D. Robertson, "Camera calibration from vanishing points in images of architectural scenes," Proceedings of the British Machine Vision Conference, vol. 2, pp.382-391, 1999.

[9] K. Daniilidis, J. Ernst, "Active intrinsic calibration using vanishing points," Pattern Recognition Letters, vol. 17, no. 11, pp.1179-1189, 1996.

[10] M. Fleck, "Perspective projection: the wrong imaging model," Technical Report, Comp. Sci., U. Iowa, 1995.

[11] C. B. Burchardt, K. Voss, "A new algorithm to correct fish-eye and strong wide-angle lens distortion from single images," Proceedings of the IEEE International Conference on Image Processing, vol. 1, pp.225-228, 2001.

[12] F. Schaffalitzky, A. Zisserman, "Planar grouping for automatic detection of vanishing lines and points," Image and Vision Computing, vol. 18, no. 9, pp.647-658, 2000.